

Characterising Human Mobility Patterns over a Large Street Network

Bin Jiang ⁽¹⁾, Junjun Yin ⁽¹⁾ and Sijian Zhao ⁽²⁾

⁽¹⁾Division of Geomatics, Department of Technology and Built Environment
University of Gävle, Sweden
Email: bin.jiang@hig.se, yinjunjun@gmail.com

⁽²⁾College of Resources Science and Technology, Beijing Normal University, China
Email: scanzhao@hotmail.com

Although remaining a controversy and requiring further and closer scientific scrutiny [1], Lévy flight behaviour has been found in a diverse variety of animal mobility and dispersals [2] [3] [4] and it becomes an appealing random walk model for animal mobility. Recently, human mobility has been found to follow the same random walk model based on the massive moving trajectories of dollar bills [5], and mobile phones [6], which can be approximated as human movement, as well as based on more accurate GPS data capturing trajectories of human movement [7]. However, our knowledge of the mechanisms governing the scale free and fractal-like mobility patterns remains limited. Here we analyse over 72 688 people's moving trajectories obtained from 50 taxicabs during a six-month period over a large street network involving four cities or towns, and illustrate that human daily mobility demonstrates scaling properties in terms of both trail (mobility from origin to destination) length and flight (mobility from one street to another) length. The trail length and flight length are best described by power law distributions. The scaling property of flight length together with a Gaussian-like distribution of turning angle indicates that human daily mobility resembles a Lévy flight. We further simulate human mobility using enormous random walkers based on agent-based simulations. It is found that (1) the simulated human mobility can reproduce the same scaling property, and (2) the simulated mobility rate correlates pretty well (R square up to 0.87) with the observed one. Further investigation illustrates that the synthetic trails generated from all pairs of origins and destinations exhibit heavy-tail distributions. These findings illustrate the possible mechanism governing the scaling properties. It is the scaling of both the underlying street network and spatial distribution of the origins and destinations that governs the scaling properties of human mobility patterns.

Human mobility, either pedestrians or vehicles, consists of enormous flights (or jumps) from one street to another and enormous walks along individual streets. To be specific, a person once she is in her origin (O) with street A will randomly (sometimes with a priority to the most connected ones) decide to choose a connected street B; she walks along street A, before she reaches the junction of A and B. Then she will choose another connected street C, and so on and so forth until she has reached her destination (D) (see the Supplementary Information on Figure S2). Thus human mobility over a street network, or network-constrained movement, sounds like a frog jumping from one street to another at the topological level, and like a turtle walking persistently along individual streets at the geometric level (see the Supplementary Information on the algorithms for simulating human mobility). This behaviour might be over simplified, because human mobility in reality tends to be purposive with destinations such as schools, offices, and homes, or to be capricious without any purpose. This mixed purposive and capricious nature of human mobility makes it very difficult for predicting individuals' trajectories, but remains unaffected on the overall traffic distribution at a collective level. In other words, human mobility is no different from the random mobility of animals in terms of the overall traffic distribution across a street network. This is the basic hypothesis we intend to verify in this letter.

The fundamental idea behind this hypothesis can be further addressed by how intensive a street is used by vehicles. By street, we refer to it as a set of consecutive street segments that can be naturally perceived as a street with a good continuity – the natural street [8] [9] or the self-organized natural street [10]. Suppose that every vehicle over a street network is equipped with a global positioning system (GPS) receiver, recording a signal every 10 seconds of the vehicle's position (x_i, y_i, t_i) along a street. How intensive a street is used by vehicles can be approximated by the number of the recoded positions along the street. Of course, the number of the positions should be adjusted by the speed effect, i.e., the faster the speed, the less the number of the positions (see the Supplementary Information on adjustment for the speed effect). The number of the recorded positions over a sufficiently long time period (e.g., one day) across a street network reflects the intensity of street use or traffic distribution over individual streets. The intensity or traffic distribution constitutes a human mobility

pattern over the street network. Now let us assume something different. Suppose that we set the same number of social insects and let them move around arbitrarily (see the above behaviour description; see also the Supplementary Information on the algorithms for simulating human mobility) over the same street network. Would the mobility pattern formed by the social insects be different from the one created by human beings? Our primary answer to the question is no. To put it differently, the mobility pattern formed by the social insects is surprisingly the same as the one by human beings.

Two data sets are involved in this study: GPS data of 50 taxicabs' positions obtained automatically from GPS receivers and anonymised customer data as to when they are picked up and dropped off. They were collected from four cities or towns in the middle of Sweden: Gävle, Sandviken, Storvik, and Hofors (see the Supplementary Information on Figure S1). The GPS data are represented by a triple (x_i, y_i, t_i) , recording the position (x_i, y_i) at time t_i , while the customer data are represented by a pair (t_p, t_d) , representing pick-up time t_p and drop-off time t_d . The GPS data are massive, a GPS signal every 10 seconds during a six-month period 24/7 for every one of the 50 cabs, capturing 59 983 958 positions. The customer data cover the same period, recording anonymously in total 166 679 customers' information about pick-up and drop-off time. Using the two datasets, we extracted 72 688 valid trails. Note the difference between the number of trails and that of customers. Those invalid trails, e.g., trails lasting too long (say, more than two hours), are excluded from our analysis. Although we tried several heuristic methods to remedy invalid trails, in the end we decided to exclude the heuristically derived trails to make our findings with an unbiased (yet still large enough) sample.

We found two very striking power laws, respectively, for the trails between 3 km and 23 km, and for the trails greater than 23 km, i.e., $P(\ell_T) \propto \ell_T^{-2.5}$ ($3 \leq \ell_T \leq 23$) and $P(\ell_T) \propto \ell_T^{-4.6}$ ($\ell_T > 23$), where ℓ_T denotes trail length (Figure 1). This finding resembles the human behaviour observed by Barabási [11] about human dynamics. It is also observed that 97% of trails are in the range 3-23 km, while only 3% are greater than 23 km. The power law behaviour of the trails is drawn on a very sound examination using the Maximum Likelihood Methods (see the Supplementary Information on methods) suggested by [12]. Details of the investigation including all parameters for the goodness of fit can be found in the Supplementary Information on observation of human mobility patterns (Table S1). The two ranges (3-23 km, and >23 km) of the trails correspond, respectively, to intra-city and inter-city movements. It implies that for both intra-city and inter-city mobility each shows a scaling property.

To uncover a possible mechanism behind the scaling property, we further examine the distribution of all possible synthetic trails between the origins and destinations (O/D) (Figure 1). The synthetic trails are assumed to be the shortest paths between the pairs of O/D. The number of O/D is massive, about 25 000 in one month, generating about 312 500 000 synthetic trails using a shortest path algorithm. This number would make the power law fit test too computationally intensive. Thanks to the clustered nature of O/D, and in order to reduce the computational burden, we first applied the k-means clustering method to create 4 000 clusters from 25 000 O/D. The gravity centers of the 4000 clusters are considered to be new O/D, which are snapped into the street network for deriving $(4000 \times 4000) / 2 - 4000 = 7 996 000$ shortest paths or synthetic trails. The probability density function (PDF) of the synthetic trails are then plotted to assess power law fit. Although no very striking power laws exist with the synthetic trails, the cumulative density function (CDF) of the synthetic trails in the ranges 3-23km, and >23km does show a tendency of power law distribution (insets with Figure 1d). It is a possible mechanism that governs the power law distribution of trail length.

A flight represents part of a movement along a persistent direction in a continuous space. In the discrete space of a street network, we define a flight as part of a movement along one particular street, which could be linear or curved (see the Supplementary Information for Figure S2). We extract 578 585 flights from 72 688 trails, and find that the flights better fit a power law with an exponential cutoff, i.e., $P(\ell_F) \propto \ell_F^{-2.3} \cdot e^{-\lambda \ell_F}$ ($\lambda = 0.00004$), than any alternatives such as log-normal, exponential, and stretched exponential (the details on the goodness of fit test can be found in the Supplementary Information on observation of human mobility patterns – Table S2). The power law exponent α is between 1 and 3, indicating a Lévy flight behavior [13]. This finding conforms to previous studies about human mobility patterns [5] [6].

We believe that it is the underlying street network, or more precisely the street morphology, that governs the Lévy flight behavior. To verify this belief, we further examine the topological structure of the street network in terms of street-street intersections. First we derived 4 056 natural streets based on the every-best-fit join principle and using degree 45 as the threshold. The reason why we adopted this particular principle is because the natural

streets formed by this principle tend to be similar in the morphological structure to the named streets [14]. The generated streets are transformed into a connectivity graph in terms of which street intersects which street, a sort of street topology based on street-street intersections. Both street length and connectivity are assessed to see whether or not they follow a power law distribution. Not surprisingly, the underlying street topology demonstrates a power law distribution with the exponent around 2.5 (more precisely 2.6 for street connectivity and 2.4 for street length) (Figure 2 and Table S2). This statistical regularity can be expressed by the 80/20 principle: 80% of less connected streets below the average, and 20% of well connected streets above the average [15]. The recorded taxicabs' positions every 10 seconds are overlapped with the streets to get an overall traffic distribution. We illustrate the fact that a minority of streets account for a majority of traffic [16], but with the current study it is fine-tuned to be 10% of well connected streets account for 90% of traffic (see the Supplementary Information on Figure S5 and Table S3).

If it is the underlying street network that determines the Lévy flight behavior, then there is no difference between human beings and social insects in forming the mobility patterns. To verify this, we further simulate human mobility based on the random behavior described at the beginning of the letter. We set 500 random walkers to move at a persistent speed of 18 km/h for 5×10^6 seconds (see the Supplementary Information on simulation of human mobility). This speed is exactly 5 meters per second, which reflects the observed speed 18 km/h. From the simulated trajectories, Lévy flight behaviour is again discovered or replicated with the simulated human mobility. Surprisingly, the simulated traffic is highly correlated to the observed ones, and the relevant R square value is up to 0.87 (see the Supplementary Information on Table S6). It implies that a significant fraction of traffic flow can be accounted for by the underlying street network, and human free will has little effect on the traffic distribution.

Finally, we investigate the property of walks, the movement between two consecutive times of 10 seconds. There are 3 299 556 walks involved in the study. The distribution of walks is identical to that of speeds. We can observe that most of the walks are with speeds less than 25km/h (96%), and very few are greater than 25km/h (4%). There is no indication towards any striking power law for walks.

In summary, we investigated in this study human mobility patterns from three different perspectives: trails between O/D, flights between streets, and walks between two consecutive time instants. We found scaling properties with both trails and flights. The flights show a particular Lévy behavior in nature. More importantly, through simulation and experiments, it is illustrated that the scaling properties are attributed to the underlying street network and spatial distribution of O/D. We further conjecture that such a mechanism can be applied to human mobility patterns at a larger scale, e.g., at a country level. It is the fractal property of space itself that governs the scaling properties of human mobility patterns. Herein the space refers to man-made infrastructure such as cities, airports, train stations and highways that all bear the scale-invariance property that governs the overall human mobility patterns.

Author contributions

The research idea was conceived by BJ, data processing, analysis and simulations were done by BJ, JY and SZ and the manuscript was written by BJ.

References:

- [1] Edwards A. M., Phillips R. A., Watkins N. W., Freeman M. P., Murphy E. J., Afanasyev V., Buldyrev S. V., et al. (2007), Revisiting Lévy flight search patterns of wandering albatrosses, bumblebees and deer, *Nature*, 449, 1044 – 1048.
- [2] Viswanathan G. M., Buldyrev S. V., Havlin S., da Luz M. G. E., Raposo E. P., and Stanley H. E. (1999), Optimizing the success of random searchers, *Nature*, 401, 911 – 914.
- [3] Viswanathan G. M., Raposo E. P., and Luz M. G. E. (2008), Lévy flights and superdiffusion in the context of biological encounters and random searches, *Physics of Life Reviews*, 5, 133-150.
- [4] Sims D. W., Southall E. J., Humphries N. E., Hays G. C., et al. (2008), Scaling laws of marine predator search behaviour, *Nature*, 451, 1098 – 1102.
- [5] Brockmann D., Hufnagel L., and Geisel T. (2006), The scaling laws of human travel, *Nature*, 439, 462 – 465.
- [6] Gonzalez M., Hidalgo C. A., and Barabási A.-L. (2008), Understanding individual human mobility patterns, *Nature*, 453, 779 – 782.
- [7] Rhee I., Shin M., Hong S., Lee K., and Chong S. (2008), On the Lévy-walk nature of human mobility: do humans walk like monkey? *INFOCOM*, Phoenix, AZ, US.

- [8] Thomson R. C. (2003), Bending the axial line: smoothly continuous road centre-line segments as a basis for road network analysis, in Hanson, J. (ed.), *Proceedings of the Fourth Space Syntax International Symposium*, University College London, London.
- [9] Jiang B. and Liu C. (2007), Street-based topological representations and analyses for predicting traffic flow in GIS, *International Journal of Geographic Information Science*, xx(xx), xx – xx, Preprint, arxiv.org/abs/0709.198.
- [10] Jiang B., Zhao S., and Yin J. (2008), Self-organized natural roads for predicting traffic flow: a sensitivity study, *Journal of Statistical Mechanics: Theory and Experiment*, July, P07008, Preprint, arxiv.org/abs/0804.1630.
- [11] Barabási A.-L. (2005), The origin of bursts and heavy tails in human dynamics, *Nature*, 435, 207 – 211.
- [12] Clauset A., Shalizi C. R., and Newman M. E. J. (2007), Power-law distributions in empirical data, Preprint arxiv.org/abs/0706.1062.
- [13] Klafter J., Shlesinger M. F., and Zumofen G. (1996), Beyond Brownian motion, *Physics Today*, February, 33 – 39.
- [14] Jiang B. and Claramunt C. (2004), Topological analysis of urban street networks, *Environment and Planning B: Planning and Design*, 31, 151- 162.
- [15] Jiang B. (2007), A topological pattern of urban street networks: universality and peculiarity, *Physica A: Statistical Mechanics and its Applications*, 384, 647 – 655.
- [16] Jiang B. (2008), Street hierarchies: a minority of streets account for a majority of traffic flow, *International Journal of Geographical Information Science*, x, xx-xx, Preprint, arxiv.org/abs/0802.1284.

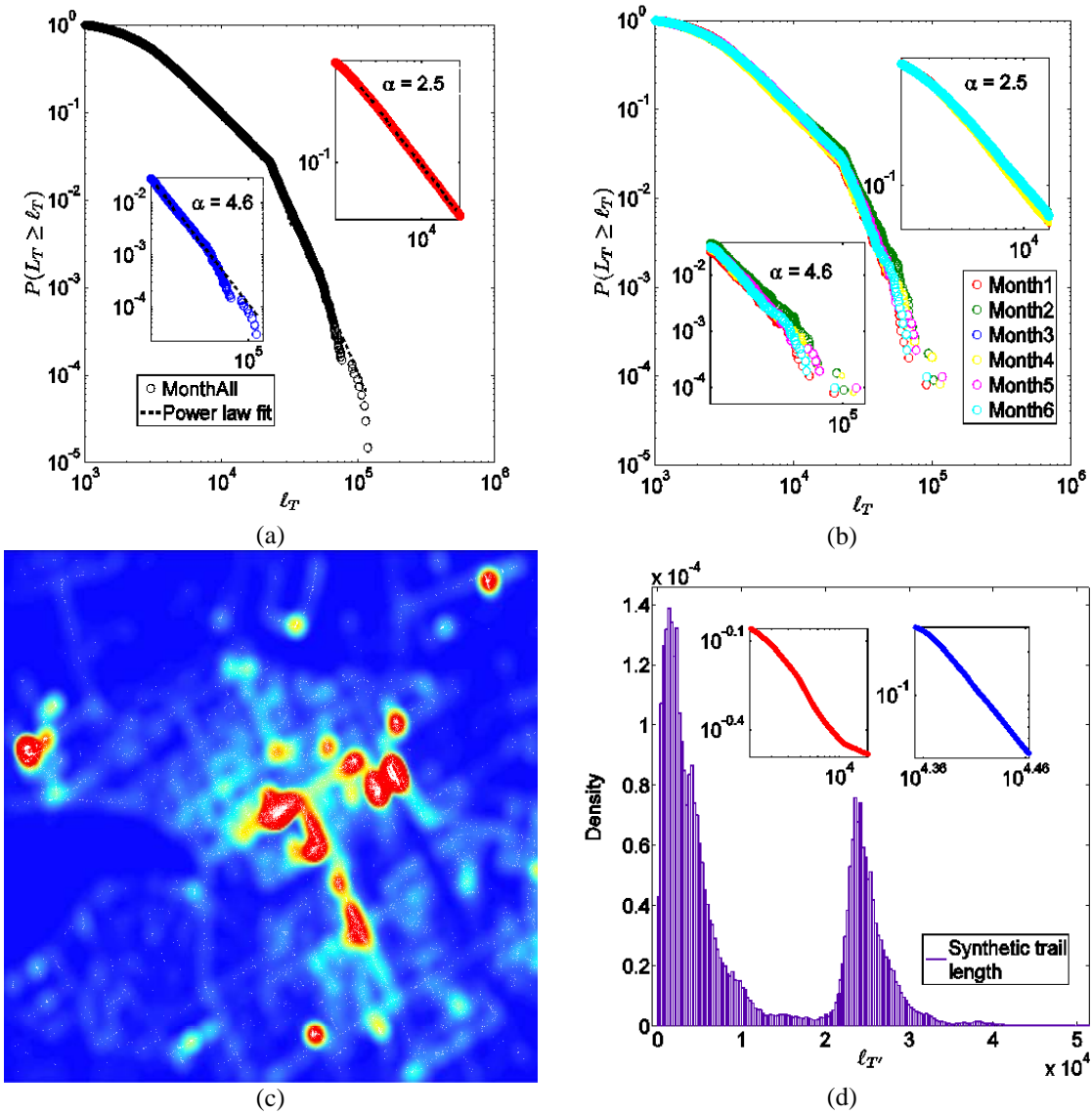


Figure 1: Scaling with trail length and a possible mechanism behind it. (a) Bipartite power law distribution for the trails of 3-23 km and >23 km for all six-months together, (b) The same power law distribution plotted month by month for consistent checking, (c) The tiny white spots are O/D during January 2008 at the centre of Gävle city. The density of O/D is visualized in color from the highest (red) to the lowest (blue). The largest red hotspot in the center is the downtown square, and other hotspots are a hospital, the central station, a district center, and the location of the taxi company. There are about 25 000 O/D in one month, which are aggregated into 4000 clusters using the k-means clustering method. These clusters are further snapped into the underlying street network for deriving synthetic trails. It is observed that about 80% of O/D are scattered, while 20% of them, indicated in red, are highly clustered, showing a clear scale-invariance and fractal property. It is the scale free nature of O/D distribution that underlies the power law distribution of trail length. (d) The PDF of the 7 996 000 synthetic trails generated from the 4000 clusters, and the CDF of the trails in the ranges of 3-23 km (inset in red), and >23 km (inset in blue), indicating two heavy-tail distributions.

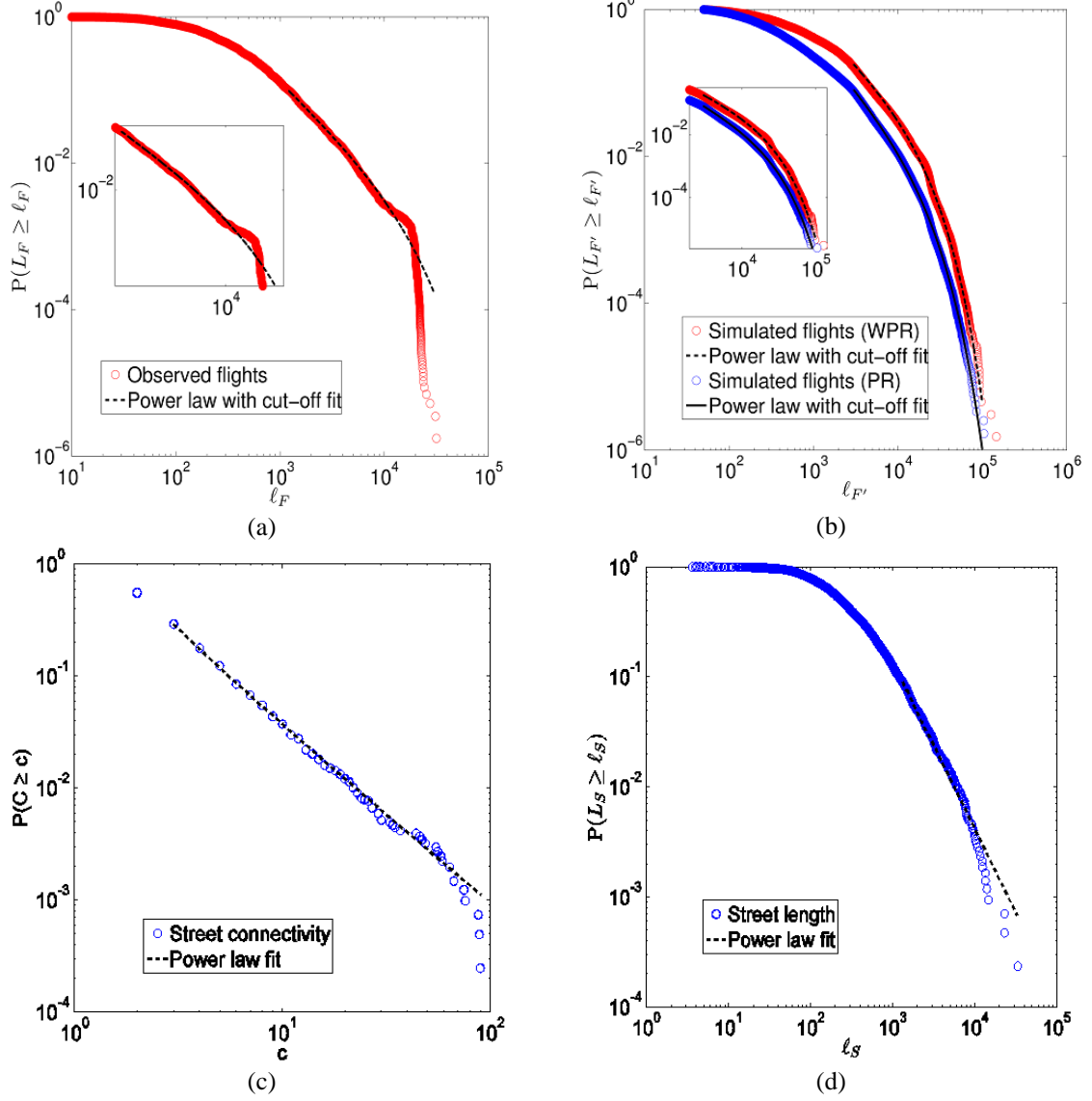


Figure 2: Lévy behavior of flights and a possible mechanism behind it. (a) Observed flights show a Lévy behavior, i.e., $P(\ell_F) \propto \ell_F^{-2.3} \cdot e^{-\lambda \ell_F}$ ($\lambda = 0.00004$), (b) Simulated flights approximately exhibit the same Lévy behavior, i.e., $P(\ell_{F'}) \propto \ell_{F'}^{-2.4} \cdot e^{-\lambda \ell_{F'}}$ ($\lambda = 0.00003$ for WPR-walkers, and $\lambda = 0.00004$ for PR-walkers), (c) The power law distribution of street connectivity, i.e., $P(c) \propto c^{-2.6}$, and (d) The similar power law distribution of street length, i.e., $P(\ell_S) \propto \ell_S^{-2.4}$, where the exponent is slightly less than that of street connectivity's distribution.

(Supplementary Information)
Characterising Human Mobility Patterns over a Large Street Network

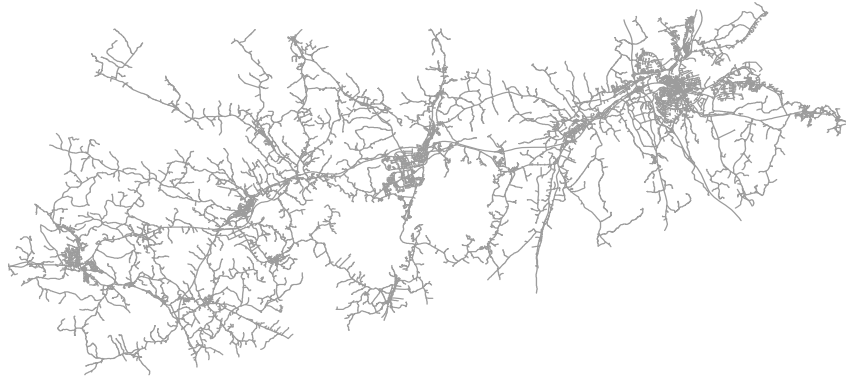
1. Data
 2. Extracting trails and flights
 3. Methods of detecting Lévy flights: fitting power laws to human movement data
 4. Observation of human mobility
 - 4.1 Power law fit for trails
 - 4.2 Power law fit for observed flights
 - 4.3 Gaussian-like distribution of the turning angle for observed flights
 - 4.4 Adjustment for the speed effect
 - 4.5 Power law fit for observed traffic (90/10)
 5. Simulation of human mobility
 - 5.1 Power law fit for simulated flights
 - 5.2 Gaussian-like distribution of the turning angle for simulated flights
 - 5.3 Power law fit for simulated traffic (90/10)
 - 5.4 Observation versus simulation
 6. Algorithms for simulating human mobility
 7. Ethical issues
- Acknowledgement**
References

1. Data

The GPS data of 50 taxicabs' positions obtained automatically from GPS receivers while the taxi services were operating over four cities or towns in the middle of Sweden: Gävle, Sandviken, Storvik, and Hofors (Figure S1a). The GPS data are massive, a GPS signal every 10 seconds during a six-month period (October 2007, January – May 2008) for every one of the 50 cabs. The customer data cover the same period, recording anonymously in total 166 679 customers' information as to when they were picked up and dropped off. Both GPS data and customer data were provided by a Swedish taxi company (TAXI Stor och Liten, www.taxi107000.com). The street data set is provided by the city of Gävle in Sweden. The total length of the streets is 2 445 kilometers over an area of 1 253 square kilometers. We generate 4 056 natural streets from in total 10 439 street segments. Note the street network covers the entire region (Figure S1b).



(a)



(b)

Figure S1: (colour online) Maps (a) the taxi service area (which is copyrighted by eniro.se), and (b) street network covering the four cities

2. Extracting trails and flights

Both GPS data and customer data were used to extract trails. From where one is picked up to where one is dropped off represents a complete movement, and the related GPS trajectory is called a trail, representing the mobility of the customer. We derive 72 688 trails from the six-month data sets. Note the difference between the number of trails (72 688) and that of customers (166 679) for some invalid trails were not counted in our statistics. The extracted trails represent a fairly true picture of human mobility, and overall traffic distribution in reality.

As shown in Figure S2, a synthetic trail passes over three different streets A, B and C, and apparently it consists of three flights. Flights have two parameters: flight length and turning angle. The turning angle is in fact the deflection angle between the corresponding adjacent street segments. For example, the turning angle between flight 1 and flight 2 is the deflection angle between street A and street B. We extract 578 585 flights from the 72 688 trails for the investigation of the Lévy behavior.

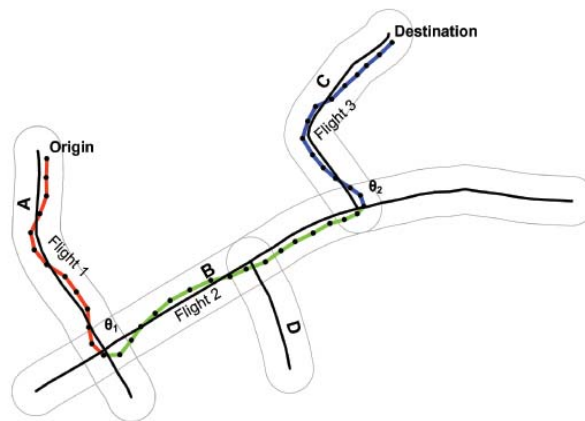


Figure S2: (colour online) Illustration of a synthetic trail and its flights

3. Methods of detecting Lévy flights: fitting power laws to human movement data

Developed by the French mathematician Paul Lévy (1886 – 1971), a Lévy flight is to extend the famous Brownian motion to be a more general random walk model (Klafter, Shlesinger, and Zumofen 1996). A random walk model is a mathematical formalization of the intuitive idea of taking successive jumps or flights, each in a random direction. Thus, the formed random walk or trajectory is characterized by two parameters: jump length and turning angle. The statistical distributions of the two parameters describe the stochastic process of a random walker. A Lévy flight is a particular random walk model that involves two different distributions: a Gaussian distribution for the turning angle (θ_i) on the one hand, i.e.,

$$P(\theta_i) \sim \frac{1}{\sigma\sqrt{2\pi}} \exp\left[-\frac{(\theta_i - \bar{\theta})^2}{2\sigma^2}\right] \quad [\text{S1}]$$

and a power law distribution for the jump length (ℓ_i) on the other, i.e.,

$$P(\ell_i) \sim \ell_i^{-\alpha} \quad [\text{S2}]$$

with $1 < \alpha < 3$.

Clearly, the distribution of the turning angle is tightly clustered around the average or means ($\bar{\theta}$), while the jump length demonstrates no means ($\bar{\ell}$). In other words, it lacks an average scale, due to which it is often called scale free. It is important to point out that the Lévy stable distribution of the sums of jump length converges to a Gaussian distribution when the Lévy exponent is set to ≥ 3 , thus indicating a Brownian motion. More significantly, Lévy flights differ from Brownian motions in movement patterns. The jump length of Brownian motions exhibits a Gaussian distribution, while that of Lévy flights possesses a power law distribution. Lévy flights consist of many Brownian clusters, connected by longer jumps between them (Figure S3).

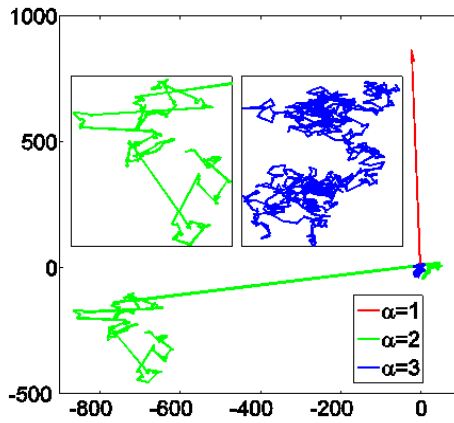


Figure S3: (colour online) Illustration of Lévy flights with different exponent α

(NOTE: $\alpha \rightarrow 1$, straight lines red; $\alpha \geq 3$, Brownian motion clusters (zoomed inset blue); $1 < \alpha < 3$, Lévy flights - Brownian motion clusters connected by longer jumps (zoomed inset green))

To detect a Lévy flight is no more than detecting a power law behavior of the jump length, i.e., to estimate the exponent α to see whether it is within the range $1 < \alpha < 3$. This is commonly achieved by plotting the histogram of jump length in logarithmic scales. When the histogram follows quite closely a straight line, we can claim a power law exists with the jump length. This can be seen clearly from the logarithmic transformation of equation [S2], i.e.,

$$\log P(\ell_i) = -\mu \log(\ell_i) + c \quad [\text{S3}]$$

where μ is the Lévy exponent, and c a constant.

However, the above commonly used method suffers from errors in the logarithmic tail of the distribution (e.g., Goldstein, Morris and Yen 2004; Newman 2005; Sims, Righton and Pitchford 2007). It looks messy at the end of the logarithmic tail because each bin has only a very few samples in it. One possible solution is to use varying width of bins in the histogram, with each bin k being increased by 2^k , to have a more homogeneous number of samples per bin. This can help to reduce errors in the tail. This method can be further refined, i.e., using the frequency per logarithmic bin normalized by dividing by bin width and total number of jumps to get the probability density (e.g., Newman 2005; Viswanathan et al. 1999). This first solution is actually based on the probability density function (PDF). Another solution, probably a much better one, is simply to use the cumulative density function (CDF), i.e., the plot of the probability that the jump length is greater than or equal to a certain value. This form of power law distribution is sometimes called Zipf's law or Pareto distribution.

The alternative solutions do not terminate here if our goal is to obtain the power law exponent. Drawing a conclusion about Lévy flight relies on an accurate estimate of the power law or Lévy exponent α . This is usually done by using least-squares fit, but it is known to introduce systematic bias (Goldstein, Morris and Yen 2004). Because of the fact that a power law distribution is likely to be confused with other heavy tail distributions such as lognormal distribution (Limpert, Stahel and Abbt 2001) and stretched exponential (Laherrere and Sornette 1998) distribution, it is very tricky to draw a power law hypothesis. Furthermore, a pure power law distribution hardly occurred with real-world data because of a limited sampling size. What is often observed with real-world data is a sort of power law with cutoff. Researchers (e.g., Goldstein, Morris and Yen 2004; Newman 2005; Clauset, Shalizi and Newman 2007) have suggested much more reliable methods, based on maximum likelihood methods and the Kolmogorov-Smirnov (KS) test, for identifying and quantifying power-law distributions. Their methods can be used not only for fitting a power law to data or part of data, but also for assessing how good the fit is, in comparison with other heavy tailed distributions. The estimated exponent is given by,

$$\alpha = 1 + n \left[\sum_{i=1}^n \ln \frac{\ell_i}{\ell_{\min}} \right]^{-1} \quad [S4]$$

where α denotes the estimated exponent, and ℓ_{\min} is the smallest jump length for which the power law holds for.

The KS test is adopted in this study to assess the goodness of fit, i.e., how human movement data fit a power law distribution. The fundamental idea is the maximum distance (D) between the CDFs of the data and the fitted model:

$$D = \max_{x \geq x_{\min}} |f(x) - g(x)| \quad [S5]$$

Where $f(x)$ is the CDF of the data with a value of at least x_{\min} , and $g(x)$ is the CDF for the power law model that best fits the data while $x \geq x_{\min}$.

With the fitted model $g(x)$, we generate 1000 synthetic datasets and recalculate the maximum distance between $f(x)$ and the fitted model, i.e., $D_i (i = 1, 2, \dots, 1000)$. We count the number of D_i whose values are greater than D, and the ratio of D_i to D is the so called p-value, reporting if the data fit the model significantly. The larger the p values, the more significant the fitted model, and p values greater than 0.01 are considered to be acceptable for a goodness of fit.

Lévy flights have been conjectured and examined by an increasing number of studies as a default model for a variety of animal movement and dispersals. Interested readers should refer to Viswanathan, Raposo and Luz (2008) and references therein for more details. The study by Viswanathan et al. (1999) and many follow-up studies (e.g., Sims et al. 2008) have shown that Lévy flights can theoretically increase the success rate of random search for a diverse variety of animals.

4. Observation of human mobility

4.1 Power law fit for trails

Table S1: Exponent α and p value for both intra- and inter-city trails (support of power law behaviour)

	Intra-city trails		Inter-city trails	
	α	p	α	p
Month1	2.69	0.02	4.73	0.20
Month2	2.45	0.04	4.44	0.85
Month3	2.48	0.49	4.63	0.03
Month4	2.57	0.22	4.68	0.15

Month5	2.54	0.16	4.72	0.44
Month6	2.52	0.09	5.05	0.51
MonthAll	2.54	0.12	4.64	0.51

4.2 Power law fit for observed flights

Table S2: Tests of Lévy flight behaviour with observed flights (support of power law with cutoff)
(LR = likelihood ratio, for more details about it, refer to Clauset, Shalizi and Newman 2007)

Flight	lognormal		exponential		stretched exp.		power law with cutoff		exponent	rate
	LR	p	LR	p	LR	p	LR	p	α	λ
Month1	-33.2	0.0	1343.5	0.0	-35.3	0.0	-45.4	0.0	2.4	0.00005
Month2	-12.4	0.0	1581.5	0.0	-13.6	0.0	-27.4	0.0	2.4	0.00003
Month3	-16.7	0.0	1503.4	0.0	-17.9	0.0	-28.8	0.0	2.4	0.00003
Month4	-34.2	0.0	1303.8	0.0	-36.8	0.0	-49.8	0.0	2.3	0.00005
Month5	-51.0	0.0	1056.8	0.0	-54.1	0.0	-64.2	0.0	2.2	0.00006
Month6	-51.0	0.0	1152.1	0.0	-53.3	0.0	-60.9	0.0	2.2	0.00006
MonthAll	-181.9	0.0	7882.7	0.0	-194.1	0.0	-260.5	0.0	2.3	0.00004

4.3 Gaussian-like distribution of the turning angle for observed flights

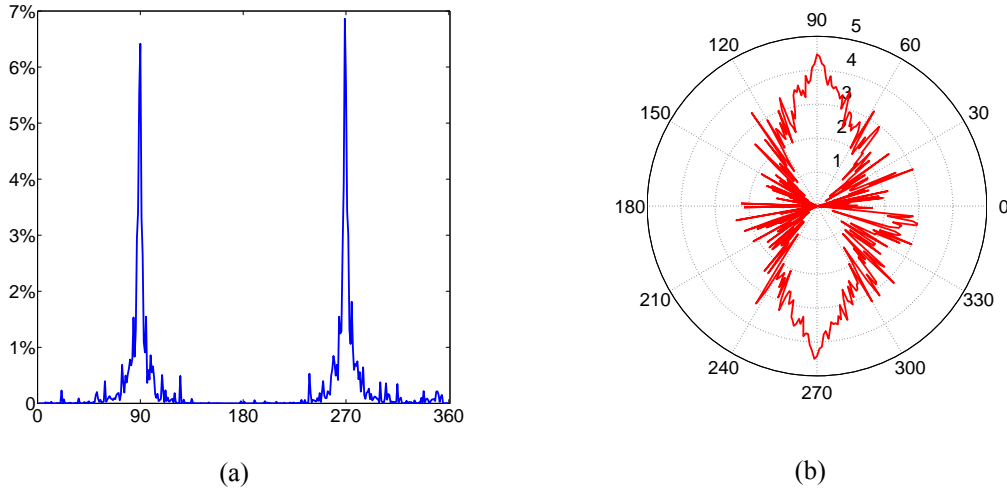


Figure S4: Gaussian-like distribution of the turning angle with the observed flights. (a) Histogram in the range of 0-360, each subrange (0-180, 180-360) showing a Gaussian-like distribution, (b) The same histogram in polar plot with logarithm for the frequency

4.4 Adjustment for the speed effect

The number of positions recorded along the individual streets indicates to a certain degree the overall traffic distribution. However, this does not consider the speed effect, i.e., the faster the speed, the less the number of the positions. In order to remove this speed effect, we made an adjustment using the equation $\# \cdot \bar{v}$, where $\#$ is the number of positions recorded in an individual street, and \bar{v} is the average speed of a cab along the street. For instance, three different cabs with speeds of 18, 7.2 and 3.6 km/h drive along a street of 100 meters, and the numbers of positions recorded would be 2, 5, and 10, respectively, given the positions are recorded every 10 seconds. After the adjustment, every cab equally contributes to the traffic distribution.

4.5 Power law fit for observed traffic (90/10)

Power law behavior is found with the observed traffic ($p=0.52$). We rediscovered that a minority of streets account for a majority of traffic, i.e., the top 10% of streets account for over 90% of traffic.

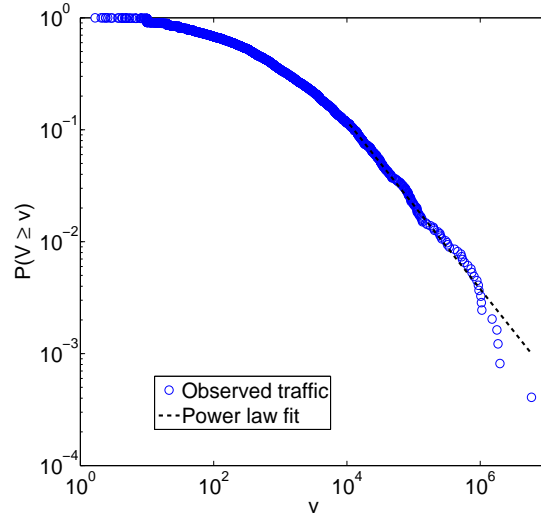


Figure S5: Power law distribution of observed traffic

Table S3: Tests of power law behaviour with observed traffic assigned to individual streets (support of power law behaviour)

	α	p
Month1	1.72	0.15
Month2	1.76	0.39
Month3	1.75	0.29
Month4	1.75	0.29
Month5	1.74	0.14
Month6	1.78	0.28
MonthAll	1.75	0.52

5. Simulation of human mobility

We simulate human mobility using an enormous number of random walkers based on the idea of agent-based simulations, in order to examine whether or not the simulation can capture the observed mobility patterns. The simulation is carried out from both topological and geometric perspectives, which are referred to as frog-like and turtle-like, respectively. For the frog-like simulation, we adopt two types of random walkers, inspired by the PageRank algorithm (Page and Brin 1998) and its modified version weighted PageRank algorithm (Xing and Ghorbani 2004), due to which they are referred to as PR-walkers and WPR-walkers. The only difference between the two types of random walkers is whether or not a priority is given in choosing the next connected streets. In other words, the PR random walkers are completely random, whereas the WPR ones are less so due to a higher priority given to most connected streets. Both the random walkers have the damping factor set to 1.0, according to our previous study (Jiang 2008). The next question is how many (N_s) random walkers are used and how long (T_s) the simulation will last, as both variables have a significant affect on the number of simulated positions. For example, when T_s is too short, or N_s is too few, most of the streets have no chance to be visited, so the simulation result would be biased. Therefore, the simulation must reach a saturated status before the simulation result can be compared against the observation. The saturated status we set is the time when the frequency of visiting the individual streets is highly correlated to the calculated PR or PWR scores. In our simulation, the correlation coefficient R square value is 0.92. This is based on the fact that the probability that a random surfer visits a web page is its PageRank. Note that the frequency of visiting individual streets and the traffic flow of individual streets are two different concepts, although they are closely related. The former is defined from the topological perspective, and it is counted only once when a connected street is chosen or visited, no matter how long the walkers move on it. However, the latter (traffic flow) is defined from the geometric

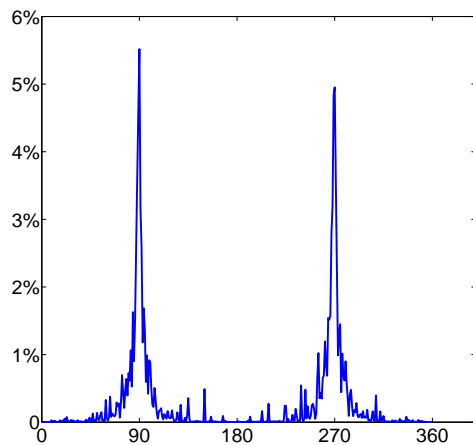
perspective, and it is accounted by how long the walkers move on it. To reach the condition of the saturated status, we set either more walkers ($\wedge N_s$) with less time ($\vee T_s$), or few walks ($\vee N_s$) with more time ($\wedge T_s$), both having the same effect.

5.1 Power law fit for simulated flights

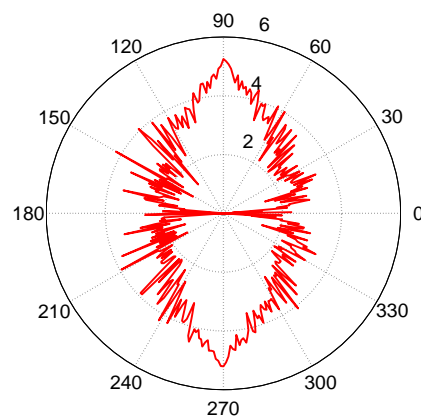
Table S4: Tests of Lévy flight behaviour with simulated flights (support of power law with cutoff) (LR = likelihood ratio, for more detail about it, refer to Clauset, Shalizi and Newman 2007; We are unable to do the test for all flights together because of the huge size, but the month cases do suggest a consistent result, i.e., support of power law with cutoff.)

	lognormal		exponential		stretched exponential		power law with cutoff		exponent	rate
	LR	p	LR	p	LR	p	LR	p	α	λ
WPR-walkers										
Month1	-915.91	0.00	12967	0	-1018	0.00	-1328.7	0	2.0847	0.00003
Month2	-838.44	0.00	13647	0	-932.9	0.00	-1242.7	0	2.12556	0.00003
Month3	-872.80	0.00	13602	0	-976.8	0.00	-1317	0	2.096245	0.00003
Month4	-894.62	0.00	13477	0	-997.3	0.00	-1319.5	0	2.094951	0.00003
Month5	-896.77	0.00	13011	0	-997.8	0.00	-1310.3	0	2.089882	0.00003
Month6	-990.32	0.00	13487	0	-1102	0.00	-1435.5	0	2.066448	0.00003
MonthAll	N/A	N/A	N/A	N/A	N/A	N/A	N/A	N/A	N/A	N/A
PR-walkers										
Month1	-548.45	0.00	7328	0	-600.8	0.00	-754.43	0	2.274887	0.00004
Month2	-578.23	0.00	7274.9	0	-634	0.00	-791.21	0	2.252193	0.00004
Month3	-665.81	0.00	6991.2	0	-726.6	0.00	-877.13	0	2.205745	0.00004
Month4	-682.51	0.00	6903.2	0	-745.1	0.00	-905.56	0	2.204626	0.00004
Month5	-604.54	0.00	6850.3	0	-666.1	0.00	-825.92	0	2.229495	0.00004
Month6	-641.62	0.00	6891.3	0	-704.9	0.00	-870.96	0	2.208273	0.00004
MonthAll	N/A	N/A	N/A	N/A	N/A	N/A	N/A	N/A	N/A	N/A

5.2 Gaussian-like distribution of the turning angle for simulated flights



(a)



(b)

Figure S6: Gaussian-like distribution of the turning angle with the simulated flights (WPR). (a) Histogram in the range of 0-360, each subrange (0-180, 180-360) showing a Gaussian-like distribution, (b) The same histogram in polar plot with logarithm for the frequency

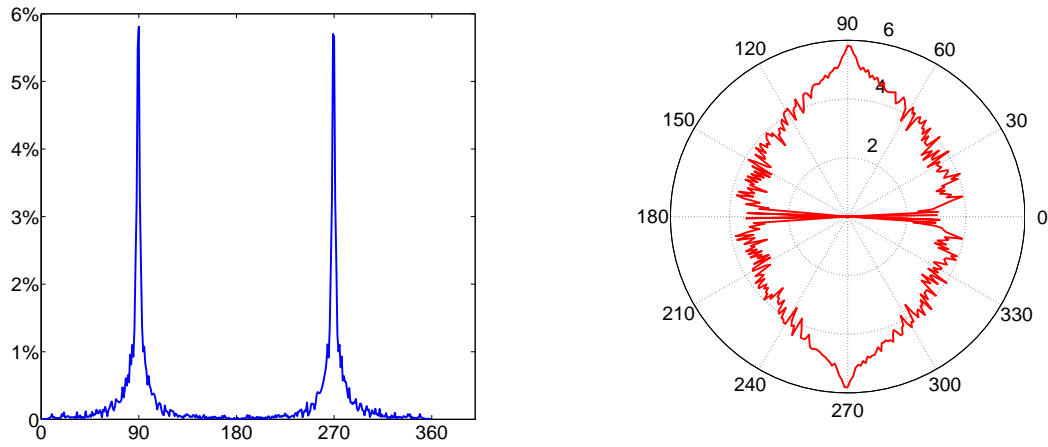


Figure S7: Gaussian-like distribution of the turning angle with the simulated flights (PR). (a) Histogram in the range of 0-360, each subrange (0-180, 180-360) showing a Gaussian-like distribution, (b) The same histogram in polar plot with logarithm for the frequency

5.3 Power law fit for simulated traffic (90/10)

Power law behavior is found with the simulated traffic (p values are 0.59, 0.11, respectively, for WPR- and PR-walkers). We rediscovered that a minority of streets account for a majority of traffic, i.e., the top 10% of streets account for over 90% of traffic.

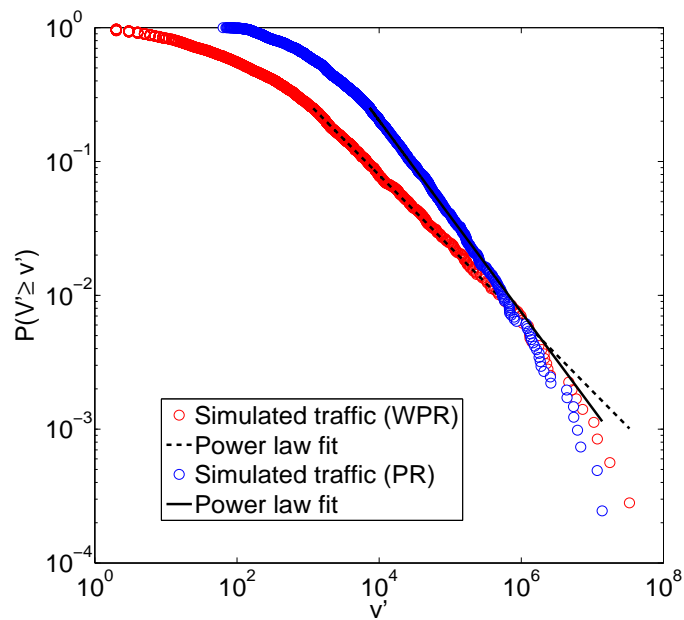


Figure S8: Power law distribution of simulated traffic

Table S5: Tests of power law behaviour with simulated traffic assigned to individual streets (support of power law behaviour)

	WPR-walkers		PR- walkers	
	α	P	α	p
Month1	1.53	0.65	1.66	0.19
Month2	1.54	0.33	1.77	0.10
Month3	1.53	0.59	1.79	0.19
Month4	1.53	0.13	1.94	0.53
Month5	1.55	0.53	1.77	0.20
Month6	1.53	0.34	1.79	0.54
MonthAll	1.54	0.59	1.72	0.11

5.4 Observation versus simulation

Table S6: R square values between observed traffic and simulated traffic assigned to individual streets (support of a significant correlation)

	WPR-walkers	PR-walkers
Month1	0.85	0.85
Month2	0.87	0.83
Month3	0.86	0.83
Month4	0.85	0.85
Month5	0.85	0.84
Month6	0.86	0.83

6. Algorithm for simulating human mobility

The algorithm is a detailed implementation of the random movement behavior given at the beginning of the letter. It is important to note a few points on the implementation: (1) each random walker arbitrarily chooses one of the observed O/D as its origin, and then follows the random behavior, (2) how long each random walker shall walk for is determined by a random generator, which generates a series of travel time (T_m) for all the walkers. The time (T_m) follows a power law distribution with an exponent of 2.5. The reason why we choose the exponent range is based on the observation of the trail length, the majority of which (97%) exhibit a power law with the exponent of 2.5.

Input: A street-based network shape file

Output: A txt file recording the number of positions in walker's trajectories for each street

Variables: D: damping factor value

T: simulation period

```

-----
//The main function of simulation
Sub Simulating()
  Transform the street-based network into a connectivity graph;
  Create N turtles distributed randomly in the OD-located streets;
  Use a power-law ( $\alpha=2.5$ ) function to randomly create a travel time  $T_m$  for each walker;
  t = 0;
  While (t <= T) do
    For Each walker in Walkers
      If the walker's real travel time >  $T_m$  Then
        Let walker jump randomly to an OD-located street;
        Use a power-law ( $\alpha=2.5$ ) function to randomly re-create a travel time  $T_m$  for it;
      End If
      Call walker::MoveOn(dt) function to let the walker move to a new location;
    Next
    t = t + dt;
  End while
  //Output
  Output the number of locations for each road to a txt file;
End sub

```

```

-----
CLASS: Walker
// Walker walking behavior
Sub Walker::MoveOn(dt)
  If (walker's next street doesn't exist) Then
    Call walker::SearchNextStreet function to get a next street;
    Get the junction between walker's current street and this street;
    If (no such junction) Then
      //Leap to another street
      Locate the walker in the middle of this street;
      Assign this street to the walker's current street;
      Increment the walker-tracked number of current street by one;
      Set the walker's next street to null;
      Return;
    Else
      Assign this street to the walker's next street;
      Compare the spatial relationship between the walker's current position and the
      junction to decide the walker's walking direction;
    End If
  End If

  Use walker's speed, direction and time increment to calculate the next position;

  If (walker reaches the junction between current street and next street) Then
    Locate the walker in the junction;
    Replace the walker's current street with next street;
    Set walker's next street to null;
    Increment the walker-tracked number of current street by one;
  Else
    Locate the walker in the new position;
    Increment the walker-tracked number of current street by one;
  End If
End sub

//Search a next street based on weighted PageRank (WPR) or standard PageRank (PR)
Function Walker::SearchNextStreet(walker's current street) as street
  Get the connected street list A from walker's current street;
  Generate a random number 0<d<1;
  If (d <= D) Then
    If (PR) Then
      Pick up a street randomly from List A;
      Return this street;
    Else if (WPR) Then
      Pick up a street from List A according to the probability p;
      // P is decided by the weight (w = connectivity / sum of connectivity)
      // this pick up is in contrast to random pick up
      Return this street;
    End If
  Else (d > D) Then
    Select a street randomly;
    Return this street;
  End If
End Function

```

7. Ethical issues

We approached the Central Ethical Vetting Committee in Sweden (Centrala etikprövningsnämnden) for ethical vetting, and were advised that there is no need for such a vetting process, as long as the data were kept anonymously, and used for research purpose.

Acknowledgement

This study is financially supported by research grants from the Hong Kong Polytechnic University and the Swedish Research Council FORMAS. We would like to thanks TAXI Stor och Liten for kindly providing the mobility data. The street network data are provided by the city of Gävle. In this connection, Anders Wahlgren and Annelie Hook deserve our special thanks for the data preparation and transferring. JY would like to thank Aaron Clauset and César Hidalgo for their advice in the KS-test.

References:

- Clauset A., Shalizi C. R., and Newman M. E. J. (2007), Power-law distributions in empirical data, Preprint arxiv.org/abs/0706.1062.
- Goldstein M. L., Morris S. A., and Yen G. G. (2004), Problems with fitting to the power law distribution, *European Physical Journal B*, 41, 255 – 258.
- Jiang B. (2008), Street hierarchies: a minority of streets account for a majority of traffic flow, *International Journal of Geographical Information Science*, x, xx-xx, Preprint, arxiv.org/abs/0802.1284.
- Klafter J., Shlesinger M. F., and Zumofen G. (1996), Beyond Brownian motion, *Physics Today*, February, 33 – 39.
- Laherrere J. and Sornette D. (1998), Stretched exponential distributions in nature and economy: ‘fat tails’ with characteristic scales, *European Physical Journal B*, 2, 525 – 539.
- Limpert E., Stahel W. A., and Abbt M. (2001), Log-normal distributions across the sciences: keys and clues, *BioScience*, 51.5, 341 – 352.
- Newman M. E. J. (2005), Power laws, Pareto distributions and Zipf’s law, *Contemporary Physics*, 46.5, 323-351.
- Page L. and Brin S. (1998), The anatomy of a large-scale hypertextual Web search engine, *Proceedings of the Seventh International Conference on World Wide Web*, 7, 107-117.
- Sims D. W., Righton D., and Pitchford J. (2007), Minimizing errors in identifying Lévy flight behaviour of organisms, *Journal of Animal Ecology*, 76, 222 – 229.
- Sims D. W., Southall E. J., Humphries N. E., Hays G. C., et al. (2008), Scaling laws of marine predator search behaviour, *Nature*, 451, 1098 – 1102.
- Viswanathan G. M., Buldyrev S. V., Havlin S., da Luz M. G. E., Raposo E. P., and Stanley H. E. (1999), Optimizing the success of random searchers, *Nature*, 401, 911 – 914.
- Viswanathan G. M., Raposo E. P., and Luz M. G. E. (2008), Lévy flights and superdiffusion in the context of biological encounters and random searches, *Physics of Life Reviews*, 5, 133-150.
- Xing W. and Ghorbani A. (2004), Weighted PageRank algorithm, *Second Annual Conference on Communication Networks and Services Research CNSR’04*, Fredericton, N.B. Canada, 305 – 314.